



Cytotoxic effect of the immunotoxin constructed of the ribosome-inactivating protein curcin and the monoclonal antibody against Her2 receptor on tumor cells

Lidia Patricia Jaramillo-Quintero, Arturo Contis Montes de Oca, Andrés Romero Rojas, Saúl Rojas-Hernández, Rafael Campos-Rodríguez & Alma Leticia Martínez-Ayala

To cite this article: Lidia Patricia Jaramillo-Quintero, Arturo Contis Montes de Oca, Andrés Romero Rojas, Saúl Rojas-Hernández, Rafael Campos-Rodríguez & Alma Leticia Martínez-Ayala (2015) Cytotoxic effect of the immunotoxin constructed of the ribosome-inactivating protein curcin and the monoclonal antibody against Her2 receptor on tumor cells, Bioscience, Biotechnology, and Biochemistry, 79:6, 896-906, DOI: [10.1080/09168451.2015.1006572](https://doi.org/10.1080/09168451.2015.1006572)

To link to this article: <https://doi.org/10.1080/09168451.2015.1006572>



Published online: 23 Feb 2015.



Submit your article to this journal [↗](#)



Article views: 357



View Crossmark data [↗](#)



Citing articles: 4 View citing articles [↗](#)

Cytotoxic effect of the immunotoxin constructed of the ribosome-inactivating protein curcin and the monoclonal antibody against Her2 receptor on tumor cells

Lidia Patricia Jaramillo-Quintero¹, Arturo Contis Montes de Oca², Andrés Romero Rojas³, Saúl Rojas-Hernández², Rafael Campos-Rodríguez² and Alma Leticia Martínez-Ayala^{4,*}

¹Centro de Investigación en Biotecnología Aplicada (CIBA-IPN), Instituto Politécnico Nacional, Tepetitla, Mexico;

²Escuela Superior de Medicina (ESM-IPN), Instituto Politécnico Nacional, Casco de Santo Tomás, Mexico;

³Facultad de Estudios Superiores Cuautitlán (FES-Cuautitlán UNAM), Universidad Nacional Autónoma de México, Cuautitlán Izcalli, Mexico; ⁴Centro de Desarrollo de Productos Bióticos (CEPROBI-IPN), Instituto Politécnico Nacional, Yautepec Morelos, Mexico

Received November 12, 2014; accepted December 17, 2014

<http://dx.doi.org/10.1080/09168451.2015.1006572>

The toxicity of the curcin on cancer cells allows to consider this protein as the toxic component of an immunotoxin directed to Her2, which is associated with cancer. Reductive amination was proposed to conjugate curcin and an anti-Her2; the binding was tested using Polyacrylamide gel electrophoresis, western blot, and immunocytochemistry. The *in vitro* cytotoxicity of curcin and the immunotoxin was assessed on breast cancer cell lines SK-BR-3 (Her2⁺) and MDA-MB-231 (Her2⁻). IC₅₀ values for curcin were 15.5 ± 8.3 and 18.6 ± 2.4 µg/mL, respectively, statistically equivalent ($p < 0.05$). While to the immunotoxin was 2.2 ± 0.08 for SK-BR-3 and 147.6 ± 2.5 µg/mL for MDA-MB-231. These values showed that the immunotoxin was seven times more toxic to the SK-BR-3 than curcin and eight times less toxic to the MDA-MB-231. The immunotoxin composed of curcin and an antibody against Her2 and constructed by reductive amination could be a therapeutic candidate against Her2⁺ cancer.

Key words: ErbB2; chemical conjugation; reductive amination; targeted therapy; breast cancer

The human epidermal growth factor receptors (ErbB or Her) are a family of four signal transduction proteins with intracellular domains that have tyrosine kinase activity. These receptors are involved in the normal regulation of cell growth, morphogenesis, and differentiation. Her2, or ErbB2, is widely expressed in epithelial cells and plays a central role in the number of cellular processes, including proliferation, motility, and resistance to apoptosis. Amplification or overexpression of Her2 disrupts normal cell control mechanisms and gives rise to aggressive tumor cells, notably in Her2 positive or Her2⁺ breast cancer (30%) and some other

cancer types (including ovarian, stomach, bladder, salivary, and lung). Overexpression of the Her2 receptor is associated with poor prognosis, aggressive tumor growth, and metastasis.¹⁾

The important role of Her2 in cancer progression and its biological characteristics make it a highly attractive target for the therapeutic treatment of cancer. Targeted therapies are transforming treatments and have already begun to make personalized medicine a reality. In fact, a monoclonal antibody (Mab) against Her2, Herceptin (also known as trastuzumab), is currently in use as a specific treatment against breast cancer.²⁾

One class of the targeted therapies is immunotoxins, which are bifunctional proteins constructed by covalently linking a Mab and a toxin. The targeting moiety recognizes and delivers the whole molecule to the specific receptors on the cell surface of the malignant cells. The toxin then triggers cell death, either by reaching the cytosol and catalytically inactivating vital cell processes or by modifying the tumor cell membrane, allowing for the selective elimination of the cells expressing the antigen recognized by the Mab.^{3–5)}

The toxins used for building immunotoxins include ribosome-inactivating proteins (RIPs), which are N-glycosidases enzymes that inhibit protein synthesis by selectively cleaving a specific adenine residue from a highly conserved structure in 28S rRNA.⁶⁾ These enzymes show depurination activity against eukaryotic and prokaryotic rRNA.⁷⁾ A broad spectrum of activities is attributed to RIPs, encompassing antiproliferative, antitumor, immunomodulatory, antiviral, antifungal, and anti-insect functions. For this reason, the interest in RIPs in possible medical and therapeutical applications is increasing. Several of these proteins have been found to be more toxic to tumor cells than to normal cells, and thus offered a theoretical opportunity for the development of antitumor drugs that selectively target tumor cells.^{8–11)}

*Corresponding author. Email: alayala@ipn.mx

To improve the selective potency, the conjugate should preferentially release the active agent in or around the tumor tissue. Thus, the characteristics of the targeting agent, the biodegradability of the linkage, and the potency of the bioactive anticancer agent are essential in the immunotoxins.^{12,13)}

Immunotoxins have evolved with time and technology and can be divided into three generations. First-generation immunotoxins were prepared by chemically coupling the whole toxins to antibodies; second-generation immunotoxins were produced by chemical conjugation but with modified toxins where the cell-binding domains were removed; and third-generation immunotoxins were made by recombinant DNA techniques and as a group are called recombinant immunotoxins.^{14,15)}

Although several authors mention that recombinant techniques are the best way to link the Mab and the toxin, the immunogenicity and clearance remain the principal inconvenience. Chemical conjugation presents a wide range of methods for conjugating proteins; however, its principal difficulty is the heterogeneity of the products.

Reductive amination is one of the most popular methods for the preparation of glycoconjugates, especially from unprotected free mono- and oligosaccharides. In brief, free aldehydes and ketones react with amines to form unstable imines or Schiff bases (reversible reaction), which are then converted to stable secondary amines using a reducing agent.¹⁶⁾ This reaction is greatly advantageous in that it does not require derivatization of the proteins and could be site-specific.

In the present study, an immunotoxin was constructed by chemical conjugation through sugar oxidation and reductive amination between the RIP curcin and the Mab against the Her2 receptor. The differential cytotoxicity of this immunotoxin was probed *in vitro* on cell lines SK-BR-3 (Her2⁺) and MDA-MB-231 (Her2⁻).

Methods

Chemical and biological materials. All of the chemicals used were of analytical research grade. Sodium periodate (NaIO₄), sodium cyanoborohydride (NaBH₃CN), ethylene glycol (C₂H₆O₂), Sephadex G-200, 3-(4,5-dimethyl-2-thiazolyl)-2,5-diphenyl-2H-tetrazolium bromide (MTT), Dulbecco's modified Eagle's medium-high glucose (DMEM), fetal bovine serum (FBS), penicillin-streptomycin solution, complete and incomplete Freund's adjuvant, the ProteoSilver™ silver stain kit, dimethyl sulfoxide (DMSO), SP-Sepharose, CM-Sepharose, and all of the salts, acids, and bases compounds used in this investigation were purchased from Sigma-Aldrich (St. Louis, MO, US). The SK-BR-3 (HTB-30) cell culture and McCoy's 5A medium (No. 30-2007) were obtained from ATCC (Manassas, VA, US). The MDA-MB-231 cell culture was a kind gift from Dr C. Ordaz (ESMyH-IPN, México). The normal human foreskin fibroblasts (BJ (ATCC CRL-2522)) cell culture was a kind gift from Dr J. Reyes (CIBIOR-IMSS, México). Reagents and materials for the electrophoresis and electroblotting methods were purchased from Bio-Rad (Hercules, CA, US). The goat anti-rabbit

IgG and anti-mouse IgG secondary antibody HRP conjugate, the glycoprotein staining kit, 4-chloro-1-naphthol, and the DAB substrate kit (3,3'-diaminobenzidine tetrahydrochloride) were purchased from Thermo Scientific (Rockford, IL, US).

Mab against Her2 receptor. The antibody against the Her2 receptor was purchased from R&D Systems. Anti-Her2 is a monoclonal mouse IgG2B clone #191924, obtained by protein A or G purification from a hybridoma culture supernatant with reactivity to human Her2. The immunogen to this antibody was the mouse myeloma cell line NS0-derived recombinant human Her2 Thr23-Thr652, accession # P04626. The anti-Her2 detects human Her2 receptor in ELISAs and western blots. This antibody does not cross-react with the other receptors of this family (EGFR, ErbB3, and ErbB4).

Curcin isolation from *J. curcas* L. seeds. Briefly, seeds of *J. curcas* L. (voucher number 2011 IZTA) were decorticated, ground, and defatted with hexane. The power was added to 1:3 (w/v) 50 mM Tris-HCl buffer, pH 7.5, 0.15 M NaCl, and continuously stirred at 4 °C overnight. The homogenate was further purified by two rounds of ion-exchange chromatography. First, the homogenate was applied to an SP-Sepharose column preequilibrated with 10 mM sodium acetate buffer, pH 4.5, followed by elution of the column with three volumes of 5 mM sodium phosphate buffer, pH 7.0 adjusted with 1 M NaCl. Next, fractions containing crude curcin were applied to a CM-Sepharose column, and curcin was eluted sequentially with a stepwise gradient of NaCl (0.3, 0.6, and 1.0 M) in 5 mM sodium phosphate buffer, pH 7.0. Finally, those fractions with curcin were pooled and dialyzed with distilled water and were concentrated using a Stirred Ultrafiltration Cell 8050 (Amicon, Beverly, MA) with a 10 kDa MWCO membrane, freeze dried and stored at -70 °C.

Physicochemical and biological characterization of curcin. The properties of curcin, including its molecular weight, isoelectric point (pI), and sequence, were determined by liquid chromatography-mass spectrometry (LC-MS). The enzymatic rRNA N-glycosidase activity of curcin was carried out using RNA from *J. curcas* L. seeds; the RNA was extracted according to Li et al.¹⁷⁾, and the enzymatic activity was done with a modified method according to Endo et al.¹⁸⁾ and Tumer et al.¹⁹⁾. The total neutral sugar content was determined using the phenol sulfuric acid method as Dubois et al.²⁰⁾, and the glycosylation of curcin was detected on a polyacrylamide gel with a Pierce Glycoprotein Staining Kit. The total protein concentration was measured by the Bradford protein assay using BSA as standard.²¹⁾

In silico modeling of curcin. To determine the availability of the glycan moiety in curcin and the feasibility of its oxidation, the three-dimensional (3D)

structure of this glycosylated protein was modeled *in silico*.

The sequence of the accession ACO53803.1 of GenBank was modeled with the I-TASSER server.²²⁾ The quality of the best curcin 3D model was inspected using the Ramachandran plot analysis.²³⁾ The predicted model was glycosylated at N-266 and N-274 according to Lin *et al.*⁸⁾ and with the oligosaccharide GlcNAc2Man3Xyl²⁴⁾ constructed using SWEET-IL.²⁵⁾ The *in silico* glycosylation was performed using the web-based tool GlyProt.²⁶⁾ Sugar oxidation was simulated by transforming the vicinal OH groups of mannose into aldehydes with MOE software, and the final model was optimized by energy minimization with MOE software.²⁷⁾

Cell cultures SK-BR-3 (Her2⁺), MDA-MB-231 (Her2⁻), and fibroblasts

The human breast adenocarcinoma cell line SK-BR-3, which overexpresses the antigen Her2 on its surface, was cultured in McCoy's 5A medium supplemented with heat-inactivated FBS to a final concentration of 10% (v/v). This cell line was cataloged as Her2⁺.

The human breast adenocarcinoma cell line MDA-MB-231, which does not overexpress the antigen Her2 on its surface, and the fibroblasts were cultured and maintained in DMEM supplemented with 10% (v/v) heat-inactivated FBS and 1% penicillin–streptomycin. The MDA-MB-231 cell line was cataloged as Her2⁻.

The cell cultures were maintained as monolayer cultures and incubated at 37 °C in a humidified atmosphere with 5% CO₂ (v/v). For all of the experiments, cells were grown to 80–90% confluence and were harvested using trypsin-EDTA.

Development of antibodies against curcin. Animals were handled in accordance with Mexican federal regulations for animal experimentation and care (NOM-062-ZOO-1999, Ministry of Agriculture, Mexico City, Mexico), with a protocol that was approved by the Institutional Animal Care and Use Committee and Institutional Ethics Committee.

Polyclonal antibodies against curcin were produced in New Zealand white rabbits. Animals were immunized with 1 mg of curcin dissolved in 1 mL of PBS, which was divided into three doses at weekly intervals. The first two immunizations were administered subcutaneously. For the first immunization, the curcin solution was emulsified with complete Freund's adjuvant, and for the second immunization, incomplete Freund's adjuvant was used. The third immunization was administered intramuscularly with the curcin solution in 3 mL of saline solution. Seven days after the last immunization, the rabbits were anesthetized with pentobarbital. Serum samples were obtained from blood extracted by cardiac puncture and stored at -70 °C.

The antibodies were purified by affinity chromatography on a Protein A column, and the anti-curcin antibody was detected by polyacrylamide gel electrophoresis (SDS-PAGE) and western blot using curcin as the antigen and an anti-rabbit IgG-HRP conjugate as the secondary antibody. The purified anti-curcin was stored at -20 °C.

SDS-PAGE and western blot analysis. SDS-PAGE was performed according to the method of Laemmli.²⁸⁾ The protein samples (20 µg) were mixed with the sample buffer either with or without 2-mercaptoethanol (ME) and heated at 100 °C for 5 min. The samples were applied to 7.5, 10, or 12% polyacrylamide gels, and electrophoretic separation was performed at 120 V for 90 min. Coomassie blue or silver nitrate was used to stain the protein bands.

To the western blot analysis, the resolved proteins by electrophoresis were electrotransferred to a 0.45 µm nitrocellulose membrane (Bio-Rad). Membranes were blocked in 10% skim milk or 1% bovine serum albumin in PBS-Tween (PBS-T) for 4 h at room temperature and then incubated in the appropriate primary antibody overnight at 4 °C. After incubation, the membrane was washed and exposed to either anti-rabbit IgG-HRP or anti-mouse IgG-HRP conjugate as the secondary antibodies. Between each step, the nitrocellulose strips were washed with PBS-T. Peroxidase activity was detected with 4-chloro-1-naphthol and H₂O₂ as the substrate.

Preparation of the immunotoxin curcin:anti-Her2 via reductive amination. The immunotoxin was constructed by linking curcin to the Mab anti-Her2 via sugar oxidation and reductive amination. Briefly, the sugars present in 5 mg of curcin were oxidized with a freshly prepared 10 mM NaIO₄ solution. Samples were incubated for 30 min at room temperature in the dark with gentle shaking, leading to the formation of reactive aldehyde groups. The oxidation was stopped with 1 mL of 0.16 M C₂H₆O₂ for 60 min in the dark at room temperature with gentle shaking. Excess reagents were removed by dialysis performed overnight at 4 °C in 0.1 M carbonate buffer pH 9.5.

The oxidized curcin was added to the anti-Her2 at a molar proportion of 5:1. The proteins were incubated for 180 min at room temperature in the dark with gentle shaking. The imine was reduced with 100 µL of 0.6 M NaBH₃CN for 120 min at 4 °C. The immunotoxin was concentrated through ultrafiltration with an Amicon Ultra-4 centrifugal filter of 100 kDa and was purified by exclusion molecular chromatography using a Sephadex G-200 column eluted with PBS.

Analysis and characterization of the immunotoxin curcin:anti-Her2. The proteins curcin, anti-Her2, and immunotoxin were analyzed by SDS-PAGE under non-reducing conditions. The union of curcin and Mab anti-Her2 was analyzed by western blot with an anti-curcin or anti-mouse IgG-HRP conjugate. The specific recognition of the conjugate by the Her2 receptor was analyzed by immunocytochemistry using the DAB substrate. The *in vitro* cytotoxicity was determined using the MTT assay.

Immunocytochemistry. SK-BR-3 and MDA-MB-231 cells were grown on glass slides and fixed with 2% paraformaldehyde for 30 min at 37 °C and then washed with PBS-T. The cells were permeabilized with Triton

0.5% for one minute and then were blocked with 6% skim milk in PBS-T overnight at 4 °C. The slides were incubated with the immunotoxin (1:250) overnight at 4 °C, washed with PBS-T, and incubated with conjugated anti-mouse IgG-HRP (1:1000) under the same conditions. The peroxidase reaction was performed in a freshly prepared DAB solution in peroxide buffer according to the manufacturer's instructions. The slides were dried and mounted for microscopic observation.

In vitro cytotoxicity assays of the immunotoxin curcun:anti-Her2. In order to probe the cytotoxic effect of the immunotoxin, the controls were the anti-Her2, the curcun, and the blocked curcun. The curcun was inactivated with the polyclonal anti-curcun antibody with the idea to block different parts of the protein and modify its conformational structure and its active site. Two milligrams of curcun were mixed with one milliliter of anti-curcun during 30 min; the solution was filtered with a 0.22 µm filter under sterilized conditions and was called blocked curcun.

The MTT assay was used to evaluate the cytotoxicity of curcun, blocked curcun, anti-Her2, and the immunotoxin curcun:anti-Her2 in the human cell lines SK-BR-3 (Her2⁺), MDA-MB-231 (Her2⁻), and fibroblasts.

The exponentially growing cells were plated in triplicate in 96-well plates (8 × 10⁴ cells/well) at a final volume of 100 µL and incubated at 37 °C for 24 h in a humidified atmosphere with 5% CO₂ (v/v). These cells were then exposed to different concentrations of curcun, blocked curcun, anti-Her2, or immunotoxin diluted in DMEM or McCoy's 5A medium and supplemented with 10% FBS and 1% penicillin–streptomycin. Plates were incubated another 24 h.

The concentrations of curcun were between 3.12 and 200 µg/mL. The concentrations of blocked curcun ranged from 15.6 to 1000 µg/mL. Anti-Her2 was dissolved in the corresponding medium at concentrations ranging from 0.7 to 45.0 µg/mL. The concentrations of the immunotoxin ranged from 0.4 to 25.0 µg/mL. All of these solutions were filtered with a 0.22 µm filter under sterilized conditions.

To measure the degree of cell proliferation after every treatment, the final viability of the cells was determined using the MTT assay (0.25 mg/mL). After 4 h of incubation under the same conditions, the MTT was removed and formazan was solubilized with DMSO. The absorbance was measured at 570 nm using the Bio-Rad Absorbance Microplate Reader.

Wells without cells and culture medium, wells with cells and culture medium, and wells with cells, culture medium, and buffer solution were used as controls. The percentages of cell survival were calculated in reference to these controls. The data were given as the means ± the standard deviation (SD) of three independent experiments, performed in triplicate. The concentration at which growth was inhibited by 50% (IC₅₀) was calculated using the GraphPad Prism software version 5.0 (GraphPad software Inc.).

Statistical analysis. The IC₅₀ results are represented as the mean ± SD and were analyzed by one-

way analysis of variance (ANOVA). Significant differences were calculated using Tukey's range test. GraphPad Prism software version 5.0 was used to analyze the data. $p < 0.05$ were considered to be significant.

Results

Physicochemical and biological characterization of curcun. The curcun isolated from *J. curcas* L. seeds was determined to have a molecular weight of 32.7 kDa, a pI of 8.70 and 4.14% sugar contents. The glycosylation of this RIP was confirmed in polyacrylamide gels with the periodic acid-Schiff method provided by the Glycoprotein Staining Kit. A very clear magenta band was produced at a molecular weight above 26 kDa and corresponding to curcun. The band is marked with an arrow in Fig. 1.

The sequence analysis showed a homology of 74.06% between curcun and the protein with accession number K9JF38 from the UniProt PDB database. This accession number corresponds to a rRNA N-glycosidase protein from *J. curcas* (Barbados nut). The enzymatic activity of curcun was confirmed using RNA from *J. curcas* L. seeds. According to Endo et al.¹⁸, the aniline treatment on RNA incubated with a RIP induces strand scission on the sites where N-glycosidase activity took place and the α-fragment is generated. In this investigation, the α-fragment of approximately 500 nucleotides was visualized on an agarose gel, when the RNA was incubated with curcun and treated with aniline.

The glycosylation, molecular weight, pI, and sugar content data are in accordance with the values reported by Stirpe²⁹ for RIPs and Lin et al.³⁰ for curcun.

In silico modeling of curcun

BLASTp at NCBI [31] was used to search for similarities between the amino acid sequence of curcun (accession number ACO53803.1) and other proteins, showing an absence of templates with more than 40% identity. Thus, the 3D structure of curcun was modeled using the I-TASSER server (Fig. 2). The complete sequence of curcun was obtained from ten threading templates that all belonged to the RIP family. The best predicted structure of curcun had a C-Score of -1.01

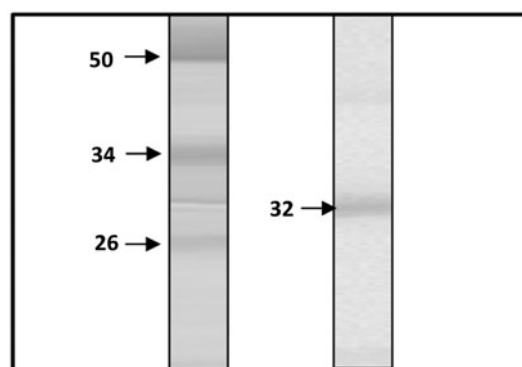


Fig. 1. Glycosylation of curcun on a reducing 12% SDS-PAGE. Notes: Lane 1: Mass molecular marker; lane 2: 10 µg of curcun (Glycoprotein Staining Kit, Thermo Scientific Co.).

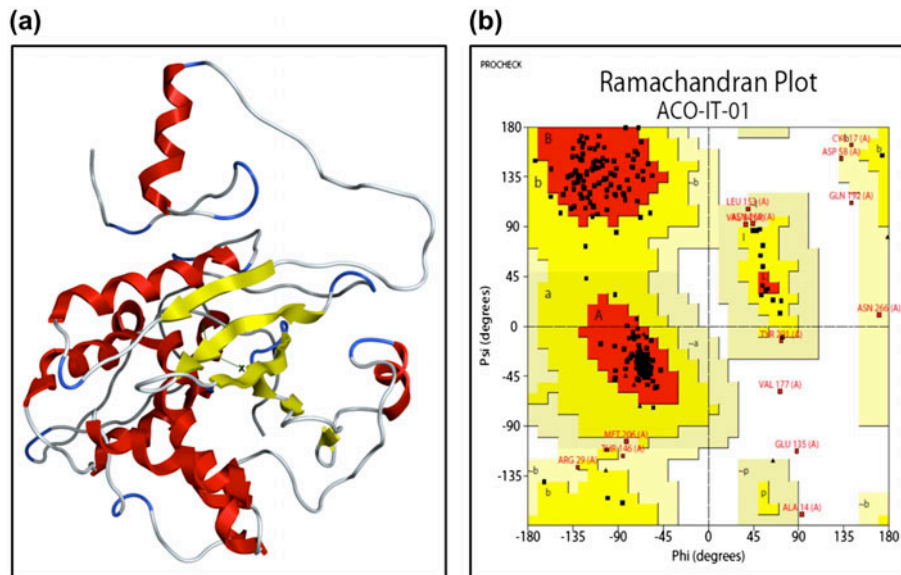


Fig. 2. Schematic representation and Ramachandran plot of the 3D structure of curcin accession number ACO53803.

Notes: (a) Schematic representation of the 3D structure of curcin accession number ACO53803.1 (I-TASSER server). Red: alpha helix; yellow: extended beta; blue: turn; white: coil. (b) Ramachandran plot of 3D model of curcin accession number ACO53803.1. The most favored regions are colored red; allowed regions are colored yellow; generously allowed regions are colored light yellow; and disallowed regions are white (PRO-CHECK analysis).

and a TM-Score of $0.59 + 0.14$. The Ramachandran plot of this 3D curcin model indicated that 94.2% of the amino acid residues were placed into the favored and allowed categories, supporting that the model has high stereochemistry and conformational structure quality (Fig. 2).

The oligosaccharide GlcNAc2Man3Xyl was constructed, and the web-based tool GlyProt was used to place this structure in the 3D model of curcin (Fig. 3). At this point, glycosylated curcin was energy minimized with MOE software, and a RMSD deviation of 1.73 Å was observed by superimposition of minimized curcin and cucurmosin (Type I RIP from *Cucurbita moschata*).

Preparation, analysis, and characterization of the immunotoxin curcin:anti-Her2

The oxidation of the sugar in curcin with NaIO_4 was followed by SDS-PAGE, which demonstrated that there was no auto-conjugation between curcin molecules. In addition, the aldehydes groups were analyzed with the Tollens' test over the course of the oxidation, with positive results for this functional group.

The immunotoxin, antibody, and curcin were electrophoresed on a 10% polyacrylamide SDS gel under non-reducing conditions, followed by Coomassie staining. Conjugation was confirmed by a shift in the electrophoretic mobility of the immunotoxin to approximately 250 kDa (lane 3 in Fig. 4) relative to oxidized curcin (32.7 kDa, lane 1 in Fig. 4) and the anti-Her2 antibody (130 kDa, lane 2 in Fig. 4).

The conjugation between curcin and the anti-Her2 was validated by western blot, with a primary rabbit anti-curcin and a secondary goat anti-rabbit or anti-mouse IgG-HRP conjugate (Fig. 5).

Curcin was detected in the curcin control (lane 1) and in the immunotoxin (lane 5), but it was not detected in anti-Her2 (lane 3). Anti-Her2 was detected

in anti-Her2 control (lane 4) and in the immunotoxin (lane 6), but not in curcin (lane 2). According to the molecular mass marker (M), curcin was detected at approximately 30 kDa (lane 1) and 250 kDa (lane 6), and anti-Her2 was detected above 130 kDa (lane 4) and 250 kDa.

One of the most important characteristics of the immunotoxins is the recognition of the antigen on the target cell. To confirm this property in the curcin: anti-Her2 construct, cultures of SK-BR-3 and MDA-MB-231 were incubated with the immunotoxin curcin: anti-Her2, and the interface between the antibody and antigen was evaluated using the chromogen DAB.

The SK-BR-3 cells were surrounded by a brown color, while the MDA-MB-231 cells did not present this color (Fig. 6). This result proved that the curcin: anti-Her2 immunotoxin recognized and attached to its antigen in Her2⁺ SK-BR-3 cells and not in the Her2⁻ MDA-MB-231 cells.

In vitro cytotoxicity assays of the immunotoxin curcin:anti-Her2

After checking the connection between curcin and anti-Her2 and the differential recognition of this conjugate toward both cell lines, the cytotoxic effect of the conjugate was evaluated.

To verify whether the cytotoxic effect was caused by the toxin curcin attached to the immunotoxin, the negative controls were blocked curcin and the anti-Her2. Curcin was blocked with the anti-curcin polyclonal antibody.

The effects of curcin on cell viability were the same in SK-BR-3 and MDA-MB-231 cell cultures at all concentrations (3.12–200 µg/mL) (Fig. 7(a)). These results were in agreement with the IC_{50} values, which were 15.5 ± 8.3 for SK-BR-3 and 18.6 ± 2.4 µg/mL for MDA-MB-231 ($p < 0.05$) (Table 1). It was evident that curcin was less toxic to the healthy cells fibroblasts

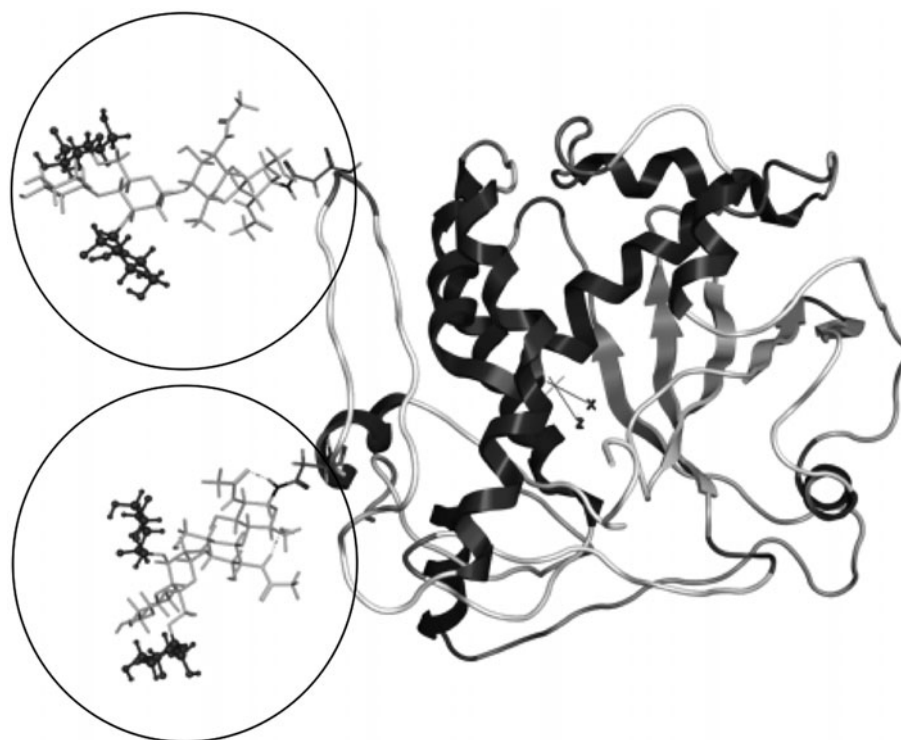


Fig. 3. Schematic representation of glycosylated curcumin showing the glycan GlcNAc2Man3Xyl at positions N-266 and N-274 (GlyProt).
Notes: Circles: Oligosaccharide moiety with four mannose residues.

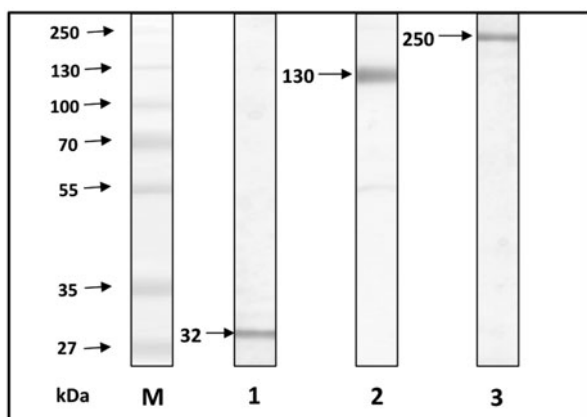


Fig. 4. SDS-PAGE analysis during construction of the immunotoxin curcumin:anti-Her2.

Notes: Coomassie stained 10% non-reducing polyacrylamide gel of oxidized curcumin with NaIO_4 (32.7 kDa, lane 1), anti-Her2 (130 kDa, lane 2), and immunotoxin curcumin:anti-Her2 (250 kDa, lane 3). M: molecular mass marker.

even at the highest concentration, with an IC_{50} value of $353.4 \pm 41.9 \mu\text{g/mL}$. In contrast, the blocked curcumin presented a differential effect between the cancer cell cultures: at all concentrations (15.6–100.0 $\mu\text{g/mL}$), the viability of SK-BR-3 cells was lower than MDA-MB-231 (Fig. 7(c)), with IC_{50} values of 184.7 ± 4.6 and $708.6 \pm 19.9 \mu\text{g/mL}$, respectively ($p < 0.05$); the fibroblasts were less affected by blocked curcumin, and since 500.0 $\mu\text{g/mL}$ of this protein the cytotoxic effect was markedly decreased, with an IC_{50} of $1079.0 \pm 21.0 \mu\text{g/mL}$ (Table 1).

By contrast, the anti-Her2 Mab did not affect both cancer cell cultures at all the concentrations (0.7–45 $\mu\text{g/mL}$). This effect was the same in both SK-BR-3

and MDA-MB-231 (Fig. 7(d)), and the IC_{50} values were 247.3 ± 26.1 and $291.3 \pm 19.8 \mu\text{g/mL}$, respectively. However, the anti-Her2 had an important cytotoxic effect on fibroblasts since 11.25 $\mu\text{g/mL}$ with 78.6% of cell viability until 45.0 $\mu\text{g/mL}$ with 55.4% of cell viability. This effect was corroborated with the IC_{50} value of $50.7 \pm 3.6 \mu\text{g/mL}$ (Table 1).

The effect of the immunotoxin curcumin:anti-Her2 on cell viability (Fig. 7(b)) was evident in the SK-BR-3 cell culture at concentrations ranging from 0.4 to 3.1 $\mu\text{g/mL}$ with 60% cell death. From these concentrations up to 25.0 $\mu\text{g/mL}$, the cell growth was slowly inhibited. The MDA-MB-231 cell culture was affected by the immunotoxin at concentrations higher than 6.2 $\mu\text{g/mL}$, but the cell growth inhibition was only approximately 17.0%. This very important differential effect of the immunotoxin was confirmed by the IC_{50} values of 2.2 ± 0.08 (SK-BR-3) and $147.6 \pm 2.5 \mu\text{g/mL}$ (MDA-MB-231) ($p < 0.05$). The cytotoxic effect of the immunotoxin on fibroblasts was very marked between 0.8 and 6.3 $\mu\text{g/mL}$, with 40.0% of cell death, but since this concentration until 25.0 $\mu\text{g/mL}$, the effect was less drastic. The IC_{50} to the immunotoxin on fibroblasts was of $16.7 \pm 2.8 \mu\text{g/mL}$ (Table 1).

Discussion

The N-glycosidase activity of curcumin used this RIP like a toxin, because it stops cell growth by inhibiting protein synthesis, while the glycosylation of this protein served as the basis for constructing the immunotoxin curcumin:anti-Her2 by reductive amination as performed in this research.

However, *in silico* analysis of a 3D model of the glycosylated curcumin structure was performed to verify

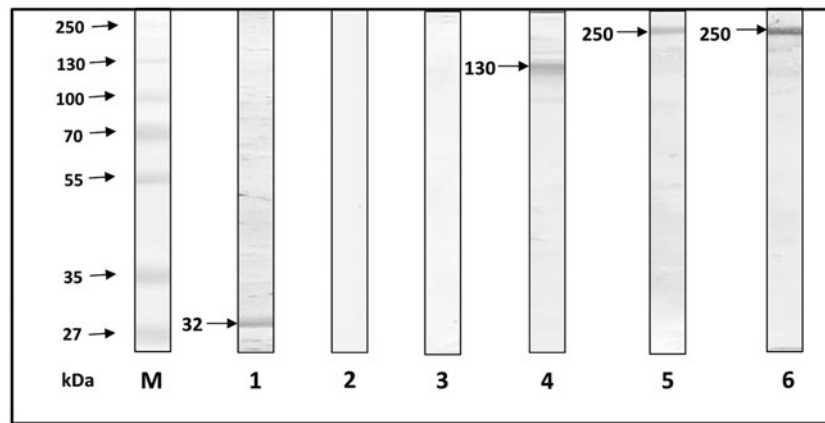


Fig. 5. Western blot analysis of a 10% non-reducing SDS-PAGE of curcin, anti-Her2, and the immunotoxin curcin:anti-Her2.

Notes: lane 1 and 2, Curcin; lane 3 and 4, anti-Her2; lane 5 and 6, immunotoxin curcin:anti-Her2. The curcin was detected with a primary rabbit anti-curcin antibody on lanes 1, 3, and 5. The anti-Her2 was detected with a secondary goat anti-mouse IgG-HRP conjugated antibody on lanes 2, 4, and 6. M: molecular mass marker.

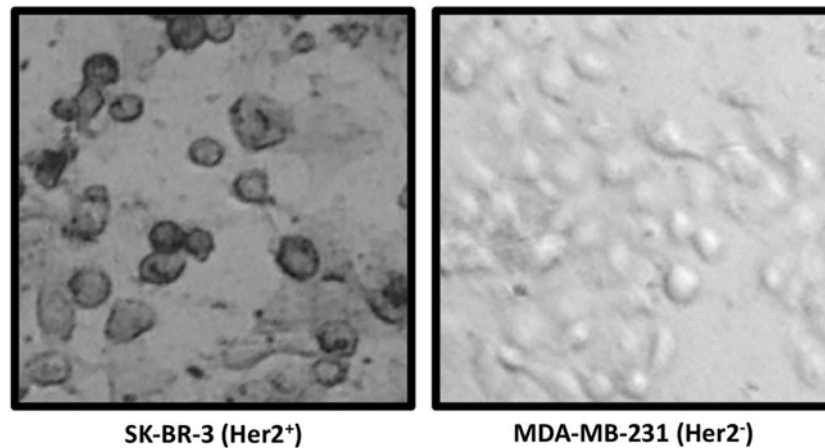


Fig. 6. Immunocytochemistry of the immunotoxin curcin:anti-Her2.

Notes: SK-BR-3 and MDA-MB-231 cell cultures were incubated with the immunotoxin (1:250) and treated with anti-mouse IgG-HRP conjugated and 3,3'-diaminobenzidine (DAB).

the glycosylation of curcin, as shown on the polyacrylamide gel, and moreover, to determine the spatial location and the availability of curcin sugars for reaction during oxidation and subsequent reductive amination.

According to I-TASSER, the best model of a predicted structure has a C-score between -5 and 2 and a TM-score higher than 0.5 . In this investigation, the best model of curcin had values for these two parameters within the ranges set by this server, ensuring good quality, correct topology, and a reliable model.

I-TASSER is a hierarchical approach for protein structure prediction that consists of template identification by multiple threading alignments, followed by tertiary structure assembly. I-TASSER uses the best multiple templates, resulting in greater query coverage and better topology, due to the TM-score-like indicator of the global topology and stronger similarity between the structures;³²⁾ besides, the quality assessment of the 3D curcin model was performed by inspection of the Psi/Phi Ramachandran plot obtained from PROCHECK analysis, a program that checks the stereochemical quality of the protein structure. I-TASSER 3D curcin model and Ramachandran plot gave and confirmed a high quality of the predicted conformational structure

model of this protein. This aspect is critically important because, ultimately, the accuracy of the model determines its suitability for specific biological and biochemical experimental designs.

According to Lin *et al.*⁸⁾, the curcin protein has two sites of N-glycosylation, at the N-266 and N-274 positions. Although the identity of the sugars has not been determined, Daubenfeld *et al.*²⁴⁾ found a glycosylation pattern of GlcNAc2Man3Xyl on gelonin (RIP) and concluded that this glycan is consistent with other RIPs. With this information, the 3D model of glycosylated curcin in Fig. 3 shows that the two asparagines with the glycan moiety are exposed and available to react. The model also shows four molecules of D-mannose (circles) with cis-diols groups that can be oxidized with NaIO_4 to create reactive aldehydes.

The information about glycosylation and possible structure and localization of the sugar moieties on curcin was essential to proceed with constructing the immunotoxin curcin:anti-Her2 through sugar oxidation on curcin and reductive amination between this protein and the anti-Her2.

The western blot and immunocytochemistry analysis confirmed the conjugation of curcin to the anti-Her2

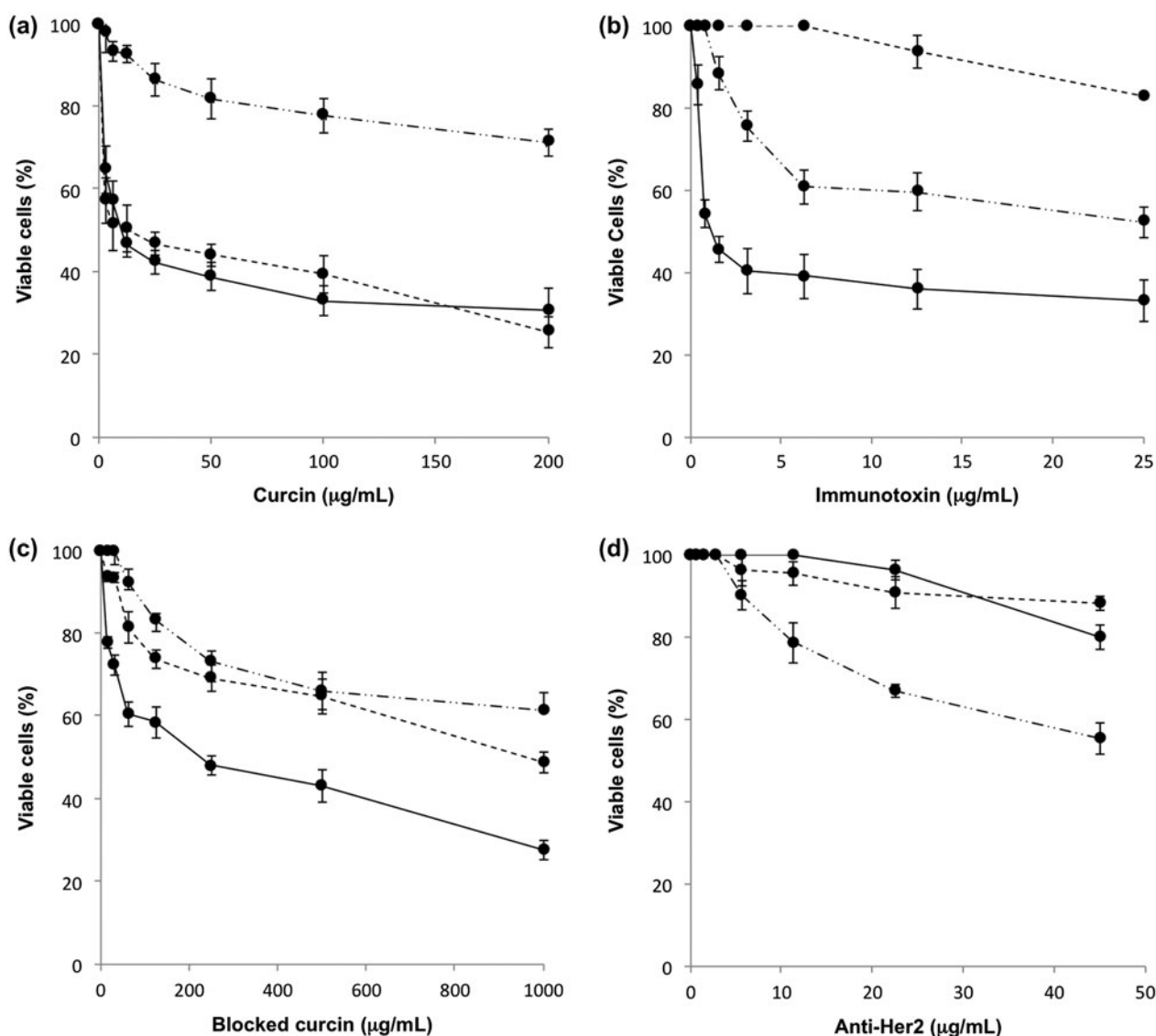


Fig. 7. *In vitro* cytotoxic activity of curcun (a), immunotoxin curcun:anti-Her2 (b), blocked curcun (c), and the antibody anti-Her2 (d) on the cell lines SK-BR-3 (—●—), MDA-MB-231 (---●---), and FIBROBLASTS (·····●·····).

Notes: The cell cultures were incubated for 24 h with different concentrations of each protein at 37 °C under a 5% CO₂ atmosphere. The viability was determined using the MTT assay. Every point is the mean ± SD of three independent experiments with three repetitions.

Table 1. Cytotoxic effects (IC₅₀) of curcun, blocked curcun, anti-Her2, and immunotoxin curcun:anti-Her2 on breast cancer cell lines SK-BR-3 (Her2⁺), MDA-MB-231 (Her2⁻), and fibroblasts.

Cell culture	IC ₅₀ (µg/mL)			
	Curcun	Blocked curcun	Anti-Her2	Immunotoxin curcun:anti-Her2
SK-BR-3 (Her2 ⁺)	15.5 ± 8.3 ^a	184.7 ± 4.6 ^c	247.3 ± 16.1 ^f	2.2 ± 0.08 ⁱ
MDA-MB-231 (Her2 ⁻)	18.6 ± 2.4 ^a	708.6 ± 19.9 ^d	291.3 ± 19.8 ^g	147.6 ± 2.5 ^j
FIBROBLASTS	353.4 ± 41.9 ^b	1079.0 ± 21.0 ^e	50.7 ± 3.6 ^h	16.7 ± 2.8 ^k

*Different letters indicate significant differences between cell cultures ($p < 0.05$).

Mab. Moreover, the specific recognition of the anti-Her2 in the immunotoxin to the Her2 receptor demonstrates that the conjugation reactions did not affect the quality of the antibody, and that it is possible to use reductive amination to conjugate proteins and construct immunotoxins.

Several authors have reported the cytotoxic effects of curcun and recombinant curcun in different types of cancer cell lines.^{8,33–36} The IC₅₀ values reported in these studies ranged from 0.23 ± 0.08 µg/mL for the gastric

cancer cell line SGC-7901⁸⁾ to 691.42 µg/mL for the hepatic cancer cell line HepG2,³⁵⁾ and even no toxic effects were observed for the HeLa cervical cancer cell line and the healthy diploid human embryo lung cell line.⁸⁾

With respect to breast cancer cell lines, Mohamed et al.³⁶⁾ reported the effect of curcun on MDA-MB-453 and MCF-7. They explored the toxicity of curcun against normal and cancer cells particularly to elucidate the biochemical and morphological events during cell

death. They reported 45% viability at 100 $\mu\text{g}/\text{mL}$ of curcun and 55% viability at 10 $\mu\text{g}/\text{mL}$ to MDA-MB-453; MCF-7 was more sensitive to curcun with 30% viability at 100 $\mu\text{g}/\text{mL}$ and around 45% viability at 10 $\mu\text{g}/\text{mL}$. These authors speculate that the cause of the difference response is the drug resistance of these cultures.

In this investigation, the breast cancer cell lines analyzed were MDA-MB-231 and SK-BR-3; both cultures are adenocarcinoma derived from metastatic site with epithelial morphology and adherent growth, and the principal difference between them is the expression of the antigen Her2. MDA-MB-231 cells lacked Her2 overexpression, whereas SK-BR-3 overexpresses this protein and is cataloged like Her2⁺. The IC₅₀ values of curcun toward breast cancer cells were 15.5 ± 8.3 for SK-BR-3 and 18.6 ± 2.4 $\mu\text{g}/\text{mL}$ for MDA-MB-231, with no significant differences between them ($p < 0.05$) (Table 1). These results showed that the Her2 receptor was not involved in the toxicity of this protein. Another important result about curcun toxicity was that this protein was not toxic to the healthy cells fibroblasts (IC₅₀ value of 353.4 ± 41.9 $\mu\text{g}/\text{mL}$). Mohamed *et al.*³⁶⁾ found this increased viability in fibroblasts treated with curcun too, and they concluded that the high mitotic index of this kind of cells could be the cause to this behavior.

The toxic effect of curcun has been attributed to its N-glycosidase activity and the inhibition of protein synthesis,⁸⁾ but since 2012, Zhao *et al.*³⁴⁾ suggested that apoptosis could be the cause of cell death. In 2014, Mohamed *et al.*³⁶⁾ reported that curcun triggered several biochemical and morphological alterations, such as mitochondrial dysfunction, nuclear degeneration, and suppression of defense mechanism, with evident alterations similar to autophagy and apoptosis, predominantly.

The ability of curcun to kill cells by apoptosis, especially cancer cells, affords the opportunity of using this RIP as a potential therapeutic agent such as an immunconjugate for the treatment of various cancers. With this objective, Zheng *et al.*³⁷⁾ fused curcun with a transferrin receptor-binding peptide (curcun-TfRBP9), and Mohamed *et al.*³⁸⁾ conjugated curcun with gold nanoparticles PEGylated and attached to folate and transferrin antibody (Au-PEG-FOL-CUR-Tfr).

With these backgrounds, the main objective of this investigation was to use this toxicity of curcun and construct an immunotoxin by directing this RIP to the Her2 receptor through an antibody directed to this antigen. Thus, the target cells were SK-BR-3, which overexpresses the Her2 antigen (Her2⁺), and the negative control cells were MDA-MB-231, with normal levels of this protein (Her2⁻).

In order to corroborate that the curcun in the immunotoxin was the toxic moiety, the blocked curcun and the anti-Her2 were probed as negative controls. Table 1 and Figs. 7(c) and 7(d) shows that the blocked curcun was not toxic to any cell line, and the anti-Her2 was not toxic to cancer cell lines; however, it was toxic to fibroblasts. This behavior is consistent with the information that the Her2 receptor is a component of the cytoplasmic membrane, and it is involved in cellular process of growth and resistance to apoptosis in healthy cells, so it is present in this kind of cells.

The toxicity of the curcun and immunotoxin (Fig. 7) and the IC₅₀ values summarized in Table 1 showed that the toxic effect of the immunotoxin was due to the curcun, because neither blocked curcun nor anti-Her2 was toxic to the cancer cell lines; that the immunotoxin had different effects on MDA-MB-231 and SK-BR-3 (Fig. 7(b)), and that the immunotoxin had differential effects respect to curcun (Fig. 7(a) and (b)).

The immunotoxin was two orders of magnitude more toxic to the cancer cell line SK-BR-3 (Her2⁺) than to MDA-MB-231 (Her2⁻) (Table 1). And comparing with curcun showed that the conjugate increased the toxicity by one order of magnitude on the SK-BR-3 cell line, while the toxicity decreased by one order of magnitude on the MDA-MB-231 cell line.

The toxin is a very important component of the immunotoxins, but antigen selection is another important factor to consider when designing these conjugates, because this determines the selectivity and the exclusive delivery of the toxin to the target cancer cells. The ideal antigen would be uniquely expressed on the cancer cell, but such antigens have not been identified. In this research, the antigen Her2 was selected because it presents two important characteristics to the objective: first, it is a cancer-associated antigen that is particularly present in breast cancer; and second, it is involved in cell regulatory processes, such as proliferation, motility, and resistance to apoptosis.

The toxicity results summarized as IC₅₀ values in Table 1 clearly show that the immunotoxin constructed through a reductive amination reaction between curcun and anti-Her2 directs the cytotoxic effect of curcun to the target cells and at lower concentrations than unconjugated curcun. The toxic effect of the immunotoxin to the fibroblasts respect to curcun could be explained, because the normal cells express the Her2 receptor.

The targeted toxicity was observed with curcun-TfRBP9,³⁷⁾ where the conjugated had significant proliferation inhibition effects on the HepG2 (liver cancer) cells that over expressed transferrin receptors, and had lower inhibitory effects on the SK-BR-3 (breast cancer) and LO-2 (normal liver) cells that expressed lower levels of this receptor; and concluded that compared with curcun, the curcun-TfRBP9 induced higher apoptosis rates in the HepG2 cells.

With respect to Au-PEG-FOL-CUR-Tfr conjugate, there was a very important and strong specificity between cancer cells (glioma) and healthy cells (HCN-1A, normal neural cells); at 100 $\mu\text{g}/\text{mL}$, glioma had 3% viability, while HCN-1A had 90% during 48 h of treatment, this results were dose-dependent and inversely proportional to the concentration of the conjugate.³⁸⁾

Besides the specificity, the immunotoxins have the clear advantage to kill cells at very low concentrations, even nanograms. It could be analyzed an important quantity of reports where immunotoxins were very potent in their lethality; however, it is difficult to compare because the RIPs and the conjugation methods were different. About conjugates of curcun, Zheng *et al.*³⁷⁾ results showed an increased toxicity (15–20%) to the curcun-TfRBP9 between 240 and 360 nM, but at higher concentrations, the difference between the conjugate and the curcun was bigger, around 30–40%.

Although the toxic effects of the Au-PEG-FOL-CUR-Tfr conjugate were very specific and dose-dependent between 1 and 100 $\mu\text{g}/\text{mL}$, the authors did not compare with curcin, so an analysis about the toxicity increment cannot be performed.³⁸⁾

The toxicity of the conjugate curcin-anti:Her2, constructed in this investigation fulfilled both characteristics of an immunotoxin, was specific to Her2 and increased the toxicity of curcin around seven times. However, the toxicity of the immunotoxin to SK-BR-3 was not as low as expected, in order of nanograms per milliliter. The possible causes of this low toxicity could be several, since the introduction of the immunotoxin to the cell until the difficulty to break the amine link between curcin and the anti-Her2. It is clear that it is important to analyze the mechanisms of entrance, movement, and degradation of this conjugate.

From 1980s to the present, immunotoxins have been constructed through the chemical coupling of a large number and variety of antibodies and RIPs, such as ricin, gelonin, saporin, PAP, and momordin. In most of these conjugates, the coupling technique was mediated by the derivatization of both antibodies and toxins with different cross-linkers reagents, such as N-succinimidyl-3-(2-pyridyldithio)-propionate (SPDP), 4-succinimidyl-oxycarbonyl- α -methyl- α -(2-pyridyldithio)-toluene (SMPT), and 2-iminothiolane (2-IT). Although most of these immunotoxins have increased toxic effects to the target cells, the heterogeneity and the instability of the disulfide bond in the molecule have limited their advance as targeted therapies.

In this investigation, the objective was to conjugate curcin and the anti-Her2 without derivatization with cross-linkers, without compromising the active sites of both molecules, and with a stable covalent bond. The conjugation was "site-directed" to the exposed mannose residues in curcin (Fig. 3) and the deprotonated ϵ -amine groups on lysine residues at pH 9.5 widely distributed across the fragment crystallizable region (Fc) of anti-Her2. The global mechanism of these reactions included the conversion of the hydroxyl groups of the mannose in reactive aldehyde groups through periodate oxidation, which reacted with ϵ -amines to form imines or Schiff bases, which were stabilized by reduction with NaBH_3CN .³⁹⁻⁴¹⁾ It is possible that this "site-specific" conjugation could reduce the heterogeneity in the structure of the conjugate both the number and position of the curcin molecules and ensures a stable amine bond.

Another way of controlling the heterogeneity of the immunotoxins is through the molar ratio between the toxin and the antibody. In this research, the molar ratio of the conjugate was 5 mol of curcin with one mole of anti-Her2. It was observed that the constructed immunotoxin had a molecular weight of approximately 250 kDa (Fig. 4). This result suggests that three curcin molecules were linked to every anti-Her2 molecule.

Clearly, future research should focus on characterizing the curcin:anti-Her2 immunotoxin and probing its effects in animal models. However, the results generated in this study and those provided by Mohamed et al.³⁶⁾ show that curcin is able to induce death of the cancer cells. Thus, it is possible that this conjugated molecule could have a high potential for use as a therapy directed against tumors Her2 positive.

Conclusions

In this investigation, reductive amination was used to construct an immunotoxin consisting of the RIP curcin and the antibody against Her2. The link between these two proteins involved the sugar residues on curcin, which were previously oxidized using NaIO_4 , and the ϵ -amine groups of the fragment crystallizable region (Fc) of the antibody to make the construct "site-specific". The immunotoxin curcin:anti-Her2 was more toxic to the SK-BR-3 cell line, which overexpressed the antigen Her2, than to the MDA-MB-231 cell line, which does not overexpress this antigen. Furthermore, the immunotoxin was more toxic compared to unconjugated curcin. The reductive amination can be a rapid and "site-specific" method for constructing immunotoxins without compromising the active sites and allowing for the action of each protein involved in this type of hybrid molecules.

Acknowledgments

We acknowledge to Consejo Nacional de Ciencia y Tecnología (CONACYT) and Instituto Politécnico Nacional (IPN) for the scholarships during the course of this investigation and to the IPN for the financial support for the research. Martínez-Ayala A.L., Campos-Rodríguez R. and Rojas-Hernández S are fellows of COFAA and EDI-IPN.

References

- [1] Tan M, Yu D. Molecular mechanisms of ErbB2-mediated breast cancer chemoresistance. In: Dihua Y, Mien-Chie H, editors. Breast cancer chemosensitivity. New York, (NY): Landes Bioscience/Springer Science+Business Media LLC; 2007. p. 119–129.
- [2] Kumar PS, Pegram M. HER2 targeted therapy in breast cancer ... beyond Herceptin. Rev. Endocr. Metab. Disord. 2007;8:269–277.
- [3] Ávila DA, Calderón FC, Pérez MR, Pons C, Pereda MC, Ortiz RA. Construction of an immunotoxin by linking a monoclonal antibody against the human epidermal growth factor receptor and a hemolytic toxin. Biol. Res. 2007;40:173–183.
- [4] Choudhary S, Mathew M, Verma RS. Therapeutic potential of anticancer immunotoxins. Drug Discovery Today. 2011;16:495–503.
- [5] Madhumathi J, Verma RS. Therapeutic targets and recent advances in protein immunotoxins. Curr. Opin. Microbiol. 2012;15:300–309.
- [6] Fracasso G, Stirpe F, Colombatti M. Ribosome-inactivating protein containing conjugates for therapeutic use. In: Lord JM, Hartley MR, editors. Toxic plant proteins 18, plant cell monographs. Berlin: Springer-Verlag; Germany; 2010. p. 225–263.
- [7] Endo Y, Wool GI. The site of action of α -sarcin on eukaryotic ribosomes. The sequence at the α -sarcin cleavage site in 28S ribosomal ribonucleic acid. J Biol Chem. 1982;257:9054–9060.
- [8] Lin J, Chen Y, Xu Y, Yan F, Tang L, Chen F. Cloning and expression of curcin, a ribosome-inactivating protein from the seeds of *Jatropha curcas*. Acta Bot. Sin. 2003;45:858–863.
- [9] Ikawati Z, Sudjadi, Sismindari. Cytotoxicity against tumor cell lines of a ribosome-inactivating protein (rip)-like protein isolated from leaves of *Mirabilis jalapa*. L. Malays. J. Pharm. Sci. 2006;4:31–41.
- [10] De Virgilio M, Lombardi A, Caliandro R, Fabbrini MS. Ribosome-inactivating proteins: From plant defense to tumor attack. Toxins. 2010;2:2699–2737.
- [11] Puri M, Kaur I, Perugini MA, Gupta RC. Ribosome-inactivating proteins: Current status and biomedical applications. Drug Discovery Today. 2012;17:774–783.

- [12] Dosio F, Brusa P, Cattel L. Immunotoxins and anticancer drug conjugate assemblies: The role of the linkage between components. *Toxins*. 2011;3:848–883.
- [13] Antignani A, FitzGerald D. Immunotoxins: The Role of the Toxin. *Toxins*. 2013;5:1486–1502.
- [14] Pastan I, Hassan R, FitzGerald DJ, Kreitman RJ. Immunotoxin treatment of cancer. *Annu. Rev. Med.* 2007;58:221–237.
- [15] Teicher BA, Chari RVJ. Antibody conjugate therapeutics: Challenges and potential. *Clin. Cancer Res.* 2011;17:6389–6397.
- [16] Farkaš P, Bystrický S. Chemical conjugation of biomacromolecules: A mini-review. *Chem. Pap.* 2010;64:683–695.
- [17] Li Z, Trick HN. Rapid method for high-quality RNA isolation from seed endosperm containing high levels of starch. *BioTechniques*. 2005;38:872–876.
- [18] Endo Y, Tsurugi K. The RNA N-glycosidase activity of ricin A-chain. *J. Biol. Chem.* 1988;263:8735–8739.
- [19] Tumer NE, Hwang D, Bonnes M. C-terminal deletion mutant of pokeweed antiviral protein inhibits viral infection but does not depurinate host ribosomes. *Proc. Nat. Acad. Sci. USA.* 1997;94:3866–3871.
- [20] Dubois M, Gilles KA, Hamilton JK, Rebers PA, Smith F. Colorimetric method for determination of sugars and related substances. *Anal. Chem.* 1956;28:350–356.
- [21] Bradford MM. Rapid and sensitive method for the quantification of microgram quantities of protein utilizing the principle of protein-dye binding. *Anal. Biochem.* 1976;72:248–254.
- [22] I-TASSER. Available from: <http://zhanglab.cmb.med.umich.edu/I-TASSER/>.
- [23] PROCHECK. Available from: <http://www.ebi.ac.uk/thornton-srv/software/PROCHECK/>.
- [24] Daubenfeld T, Hossan M, Trommer WE, Niedner-Schatteburg G. On the contentious sequence and glycosylation motif of the ribosome inactivating plant protein gelonin. *Biochem. Biophys. Res. Commun.* 2005;333:984–989.
- [25] SWEET-II. Available from: <http://www.glycosciences.de/modeling/sweet2/>.
- [26] GlyProt. Available from: <http://www.glycosciences.de/modeling/glyprot/php/main.php>.
- [27] MOE. Available from: http://www.chemcomp.com/MOE-Molecular_Modeling_and_Simulations.
- [28] Laemmli UK. Cleavage of structural proteins during the assembly of the head of bacteriophage. *Nature*. 1970;227:680–685.
- [29] Stirpe F. Ribosome-inactivating proteins. *Toxicon*. 2004;44:371–383.
- [30] Lin J, Zhou X, Wang J, Jiang P, Tang K. Purification and characterization of curcin, a toxic lectin from the seed of *Jatropha curcas*. *Prep. Biochem Biotechnol.* 2010;140:107–118.
- [31] NCBI. Available from: <http://www.ncbi.nlm.nih.gov>.
- [32] Zhang Y, Skolnick J. Automated structure prediction of weakly homologous proteins on a genomic scale. *Proc. Nat. Acad. Sci. USA.* 2004;101:7594–7599.
- [33] Luo M, Yang X, Liu W, Xu Y, Huang P, Yan F, Chen F. Expression, purification and anti-tumor activity of curcin. *Acta Biochim. Biophys. Sin.* 2006;38:663–668.
- [34] Zhao Q, Wang W, Wang Y, Xu Y, Chen F. The effect of curcin from *Jatropha curcas* on apoptosis of mouse sarcoma-180 cells. *Fitoterapia*. 2012;83:849–852.
- [35] DanDan X, Bo Z, YaDong H, QiHao Z, ZhiJian S, Hua X, Qing Z. Expression of recombinant curcin in *Jatropha curcas* L. and its anti-tumor activity *in vitro*. *Med. Plant.* 2012;3:68–71.
- [36] Mohamed SM, Veeranarayanan S, Minegishi H, Sakamoto Y, Shimane Y, Nagaoka Y, Aki A, Poulouse CA, Echigo A, Yoshida Y, Maekawa T, Kumar DS. Cytological and subcellular response of cells exposed to the type-1 RIP curcin and its hemocompatibility analysis. *Sci. Rep.* 2014;4:5747.
- [37] Zheng Q, Xiong Y-L, Su Z-J, Zhang Q-H, Dai X-Y, Li L-Y, Xiao X, Huang Y-D. Expression of curcin–transferrin receptor binding peptide fusion protein and its anti-tumor activity. *Protein Express Purif.* 2013;89:181–188.
- [38] Mohamed SM, Veeranarayanan S, Poulouse AC, Nagaoka Y, Minegishi H, Yoshida Y, Maekawa T, Kumar DS. Type 1 ribotoxin-curcin conjugated biogenic gold nanoparticles for a multimodal therapeutic approach towards brain cancer. *Biochimic. et Biophys. Acta.* 2014;1840:1657–1669.
- [39] Gildersleeve CJ, Oyelaran O, Simpson TJ, Allred B. Improved procedure for direct coupling of carbohydrates to proteins via reductive amination. *Bioconjugate Chem.* 2008;19:1485–1490.
- [40] Hermanson TG. *Bioconjugate techniques*. 3rd ed. New York (NY): Academic Press; 2013.
- [41] Kumar KR, Xiavour S, Latha S, Kumar V. Sukumaran. Anti-human IgG-horseradish peroxidase conjugate preparation and its use in ELISA and Western Blotting experiments. *J. Chromatogr. Sep. Tech.* 2014;5:211. doi:10.4172/2157-7064.1000211.